SSIM 2023 – PM Dight (ed.)

doi:10.36487/ACG_repo/2335_30

Development of a fully constrained structural model in a volcano caldera and its influence on open pit slope design

B Stoch *WSP, Australia*

T Darakjian *WSP, Canada*

L Zorzi *WSP, Canada*

S Luck *WSP, Australia*

D Luck *WSP, Australia*

K Moffitt *Equilibrium Mining, Australia*

S Nicoll *Newcrest Mining Limited, Australia*

D Tennant *Newcrest Mining Limited, Australia*

F Pothitos *Newcrest Mining Limited, Australia*

Abstract

The Ladolam gold deposit, is located on Lihir Island, part of the Tabar-Lihir-Tanga-Feni island chain, New Ireland Province, Papua New Guinea. The Luise volcano hosts the deposit, presenting a 4 × 3.5 km-wide amphitheatre, elongated and breached to the northeast. A detailed structural model of the site is required in order to incorporate the influence of structure on slope stability for pit design and optimisation. Complex tectonic evolution, late diatreme intrusion, significant metasomatic overprint, ongoing hydrothermal activity and weathering of the country rock present challenges to developing a comprehensive, fully constrained structural model across the deposit. Given this geological complexity, structural model development and structural characterisation has utilised an evidence-based approach, with inputs from numerous disparate datasets ranging from high-resolution photogrammetry to field mapping data, core logs and downhole photographs. Photogrammetry data proved highly effective in delineating deposit scale structural trends, particularly in areas that are no longer accessible or that have historically been omitted from study. Geological structures and geotechnical variations have implications for slope design and operational risk management. Strain shadows of major north–south trending structures present zones of rheological weakness and preferential fluid ingress at Lihir, further highlighting the potential influence of geological structure on slope stability. Ongoing structural characterisation has important safety and economic benefits. As the structural model is further developed, it supports the identification of potentially higher-risk areas in current slope design. This, in turn, justifies more detailed analysis or monitoring controls to ensure safe and efficient mining and/or mine design adjustments to mitigate hazards. The following work is presented in this paper: 1) the methodology used to identify and delineate key structures, 2) characterisation methodologies employed, and 3) how identification and characterisation of structural systems have successfully informed decision-making at Lihir gold mine.

Keywords: *structural geology, structural characterisation, caldera, stability analysis, geotechnical characterisation, slope optimisation, slope stability*

1 Introduction

The Ladolam deposit is located on Lihir Island, part of the young (<4 Ma) Tabar-Lihir-Tanga-Feni island chain northeast of the New Ireland Province of Papua New Guinea (Figure 1). The deposit is among the youngest (<1 Ma) gold deposits in the world (Davies & Ballantyne 1987; Moyle et al. 1990; Carman 1994).

Lihir Island is located northeast of New Ireland, Papua New Guinea, as part of the young (<4 Ma), evenly distributed Tabar-Lihir-Tanga-Feni island chain (Figure 1). The tectonic setting is complex, involving numerous rotated and transposed microplates driven principally by protracted, oblique, westward convergence of the Pacific Plate with the Australian Plate, which initiated around 50 to 42 Ma (Gordon et al. 1978; Hall 2002; Sharp & Clague 2006; Sykora et al. 2018). Volcanism may have also occurred during progressive north-westward transposition and counterclockwise rotation of the North Bismarck Plate relative to the South Bismarck Plate during the last ~3.5 Ma., possibly aided by the pre-existing island arc architecture associated from the palaeo-Melanesian subduction zone (Sykora 2016).

The Ladolam gold deposit is hosted within the Luise caldera, presenting a 4 × 3.5 km-wide amphitheatre inferred to be a remnant of the original ~1.1 km-high volcanic cone that underwent northeast-directed sector collapse and prolonged tropical weathering (Sykora et al. 2018). The ore deposit is situated in the footwall of the sector collapse detachment surface and consists of several orebodies. It contains an active high-temperature geothermal system that continues to alter rocks, cause brecciation and carry gold (Pichler et al. 1999; Simmons & Brown 2006).

Complex tectonic development, late diatreme intrusion, significant alteration overprint, ongoing hydrothermal activity and weathering of the country rock, as discussed in the following sections, present challenges to slope design. To effectively predict and account for these often-interacting factors, a comprehensive, fully constrained structural model was developed. The development of a fully constrained model entails the establishment of a structural network that conforms not only to all available data, but also the kinematic history of the deposit as it is understood. This provides a useful tool for detailed predictive slope design and sensitivity analysis.

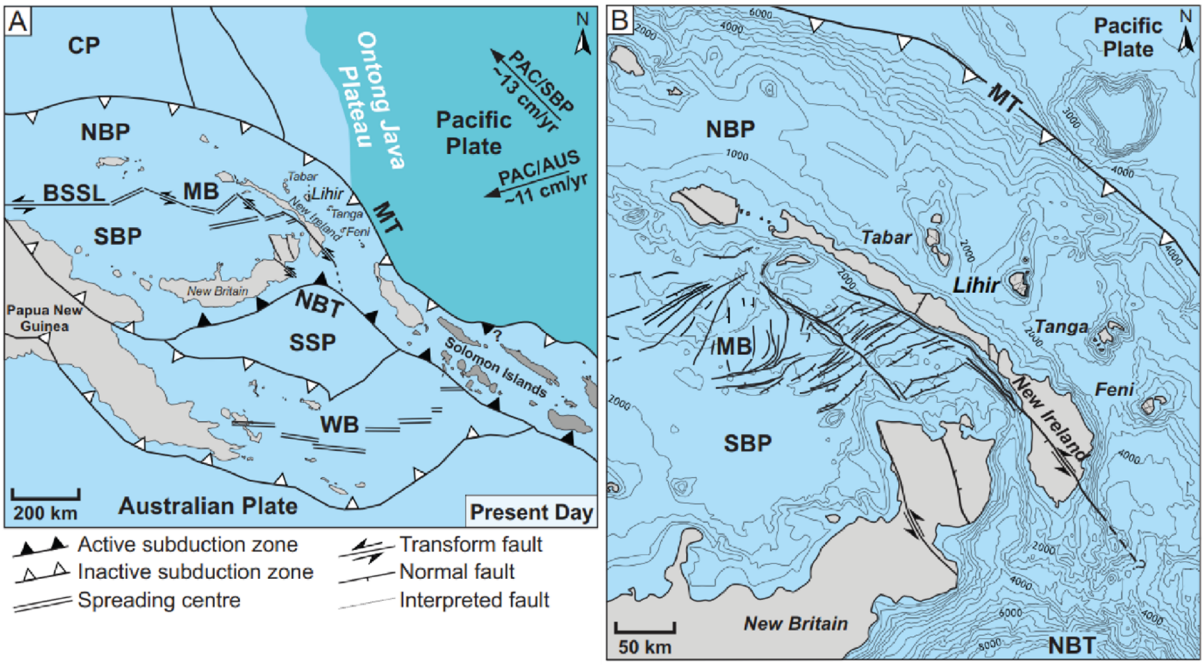

Figure 1 **Present-day location and tectonic elements around Lihir Island, Papua New Guinea, from Sykora et al. 2018. (A) Major tectonic elements around Papua New Guinea; (B) Bathymetry (500 m contour spacing) and major geologic structures around the Tabar-Lihir-Tanga-Feni island chain, New Britain and Manus Basin. Abbreviations: AUS = Australian plate, BSSL = Bismarck Sea seismic lineation, CP = Caroline Plate, MB = Manus Basin, MT = Melanesian Trench, NBP = North Bismarck Plate, NBT = New Britain Trench, PAC = Pacific Plate, SBP = South Bismarck Plate, SSP = Solomon Sea Plate, WB = Woodlark Basin**

2 Local geology

2.1 Island and deposit geology

Lihir Island is composed of volcanic lavas, volcaniclastic deposits, intrusives and fringing limestone reef deposits (Wallace et al. 1983). Three of the five mapped volcanic centres are characterised by a seaward-breached amphitheatre inferred to have formed via sector collapse; the most prominent of which is the Luise amphitheatre, host to the Ladolam gold deposit (Figure 2). The Luise amphitheatre is 4 × 3.5 km wide, and elongated and breached to the northeast. The pre-mining depth of the amphitheatre floor was 80 m relative to sea level (RSL), and the height of the walls was 640 m RSL (Blackwell 2010; Cooke & Sykora 2020). The original volcanic cone height is estimated to have been 1,100 m RSL (Wallace et al. 1983; Tregoning 2002; Blackwell 2010). The evolution of the Luise amphitheatre consisted of multiple phases of constructional volcanism and magmatism, involving basaltic to andesitic volcano-sedimentary strata and emplacement of equigranular to porphyritic intrusions (Davies & Ballantyne 1987; Moyle et al. 1990; Carman 1994; Blackwell 2010). Following volcanic sector collapse, lithostatic load was rapidly decreased, leading to the boiling of mineralised fluids and resulting in the formation of an epithermal gold deposit (Blackwell 2010). Maar-diatreme activity then continued within the caldera, leading to the formation of diatreme pipe structures and crater lake sediments.

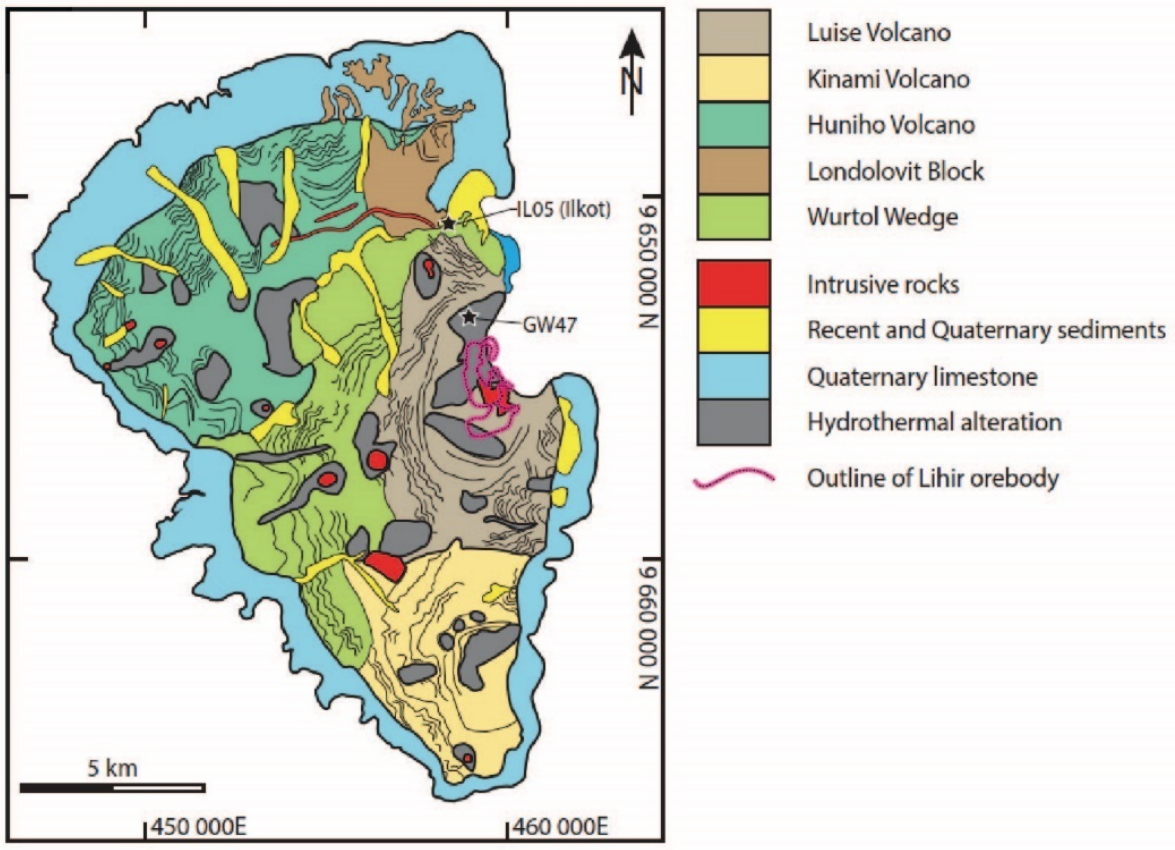

Figure 2 Geological overview of Lihir Island reporting five major volcanoclastic domains, the position of outcropping intrusive rock and broad hydrothermal alteration zones, and the outline of the Lihir gold deposit, modified after Lawlis (2020)

2.2 Hydrothermal alteration

Primary volcanic rock types at Lihir mine have been obscured by intense alteration from early to modern hydrothermal activity. Alteration is pervasive and extends vertically and horizontally beyond the Luise amphitheatre. The alteration is broadly classified into three zones, determined by type and intensity. These zones are a low-grade, steam-heated clay alteration zone near the surface, a high-grade sulfide and adularia

alteration zone, and a lower-grade zone with anhydrite, carbonate veins and biotite alteration (Blackwell 2010; Sykora 2018).

The lower anhydrite zone represents an early porphyry-style magmatic-hydrothermal stage dating back to approximately 0.9–0.3 Ma (Davies & Ballantyne 1987; Moyle et al. 1990; Carman 1994), while the sulfide-adularia zone marks a transition to an epithermal environment around 0.6–0.2 Ma, inferred to have been caused by lithostatic unloading. The surficial zone with intense clay alteration is a product of the modern geothermal system, which has been active from approximately 0.15 Ma to the present (Lawlis et al. 2015). Episodic volcanism has occurred during the modern geothermal stage, resulting in the formation of volcanic-hydrothermal breccia bodies. These breccia bodies crosscut all alteration zones and remain almost unaltered in upper diatreme materials. While the alteration zones provide a general framework, there is significant heterogeneity within them. The geothermal stage, represented by the clay zone, is relatively uniform.

Alteration zones have implications for structural interpretation and slope stability at Lihir mine, and have the following impacts:

- Strain expression is determined by rheological competency of host rock materials. For example, more competent host rock expresses strain as discrete faults while incompetent altered materials may express strain as an increase in fracture frequency or broad damaged zones.
- Gradational interface between broad alteration zones may result in reduced shear strength of structures or rock mass due to differential strength and deformation characteristics.
- Alteration affects permeability and fluid flow, resulting in porewater pressure distribution variability and locally reduced slope stability. The interaction between alteration zones and groundwater further influences pore pressure distribution and can increase the risk of shear failure along the altered areas (Holt 1990).

2.3 Structural evolution

Early northwest- and/or southeast-directed compression and west-northwest-directed extension is linked with fault and vein formation during early porphyry-style alteration under low differential stress. Protracted/multistage, northwest-directed extension was dominant for the porphyry- to epithermal-stage fault and vein development. Initial fault and vein formation was followed by modification via anhydrite dissolution, along with some block rotation and collapse brecciation (Sykora 2016; Sykora et al. 2018).

These modified veins localised some shear, and their sub-horizontal to low-angle northward-dipping orientations may have had some control over the geometry and lubrication for sector collapse events. However, structures appear not to be kinematically linked to the northeast-directed collapse events due to their top-block to the northwest or north-northwest sense of shear (Corbett 2012; Sykora et al. 2018).

High-grade epithermal-style gold mineralisation is interpreted as post-caldera collapse. Continued extension (top-block down to the northwest) continued along preferentially reactivated faults and anhydrite vein systems with low-angle dips. Faults and vein development underwent reactivation under extensional conditions. Reactivation produced northeast-striking tensile to hybrid veins (tensile and shear) and breccia veins with high-angle dips and rhombic dilational jogs, localising high-grade mineralisation (Sykora 2016; Sykora et al. 2018).

The northeast to east-northeast-striking faults, which are present at both the island scale and the deposit scale, were inherited from a tectonically generated structural grain. These faults have been reactivated throughout the evolution of the deposit. Similarly oriented deep-seated faults are considered to have contributed to the northeast elongation of the volcanic amphitheatre.

Further deformation comprises of late-stage diatreme intrusion and subsequent subsidence/collapse. The explosive nature of diatreme formation generates significant stresses, resulting in faulting and shearing along diatreme contacts, as well as post-emplacement annular gravity driven slumping (Cole et al 2005; Lawlis

2020) (Figure 3). This annular faulting is typically exacerbated where pre-diatreme structures, such as regional faults (in this case northeast to east-northeast faults) or those created during initial caldera formation, occur.

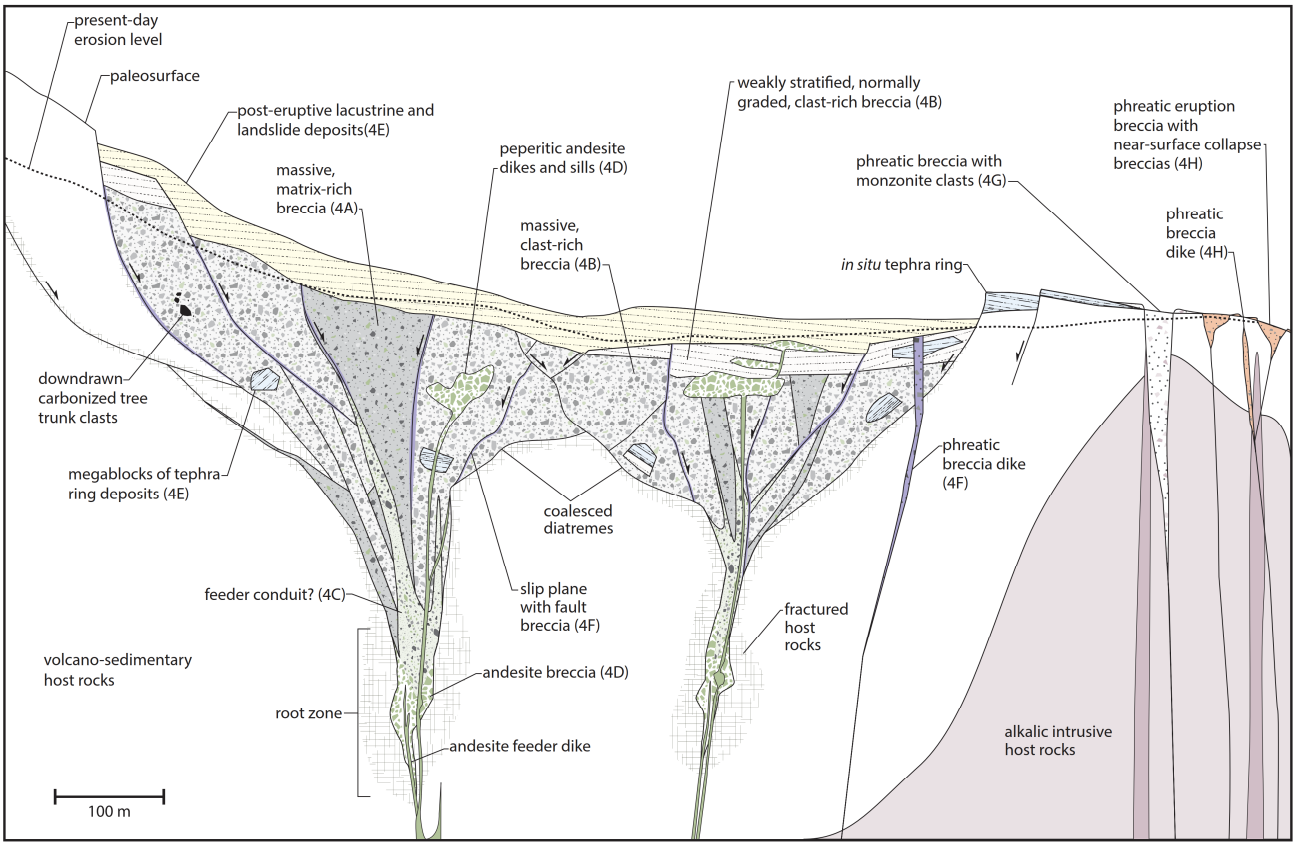

Figure 3 Examples of deformation related to late-stage diatreme intrusion and subsequent subsidence/collapse: schematic diagram of an idealised north-northwest-facing cross-section through the Lihir diatreme breccia complex, from Lawlis (2020)

3 Methodology

3.1 Data capture and interrogation

A combination of several datasets is available and has been used for the identification and interpretation of structures at Lihir mine, namely (Figure 4):

- Surface mapping (remote and physical methods).
- Downhole geophysical data, such as acoustic/optical televiewer data (ATV/OTV).
- Structural and geotechnical logging.
- Core photographs.

These datasets were interrogated to identify structures with anticipated strike extents exceeding a typical bench height (4 m). This assumption was made to focus the effort on generating a model that would highlight structures which would have an influence on the overall stability performances of the pit walls. Physical surveys, such as field mapping and geological traverses, provided contextual information to assist with the delineation and interpretation of structures from geophysical/remote techniques. Combining remote and physical surface mapping methods provides a more comprehensive understanding of the spatial relationships of interpreted structures, as well as a better constraint on the continuity and geometry of each interpreted structure.

Downhole geophysical data and macrostructural/geotechnical logging contribute greatly to defining geological structures at depth and beyond surface expression. ATV/OTV surveys offer valuable insights, allowing analysis of the orientation, size and intensity of fractures and fault systems. Downhole photography complements downhole geophysical logging techniques by providing visual documentation of the drillhole intervals, allowing workers to identify relevant structures in detail. Integrating all available datasets in the interpretation has assisted with determining stress distribution, rock mass properties and possible fluid flow pathways.

A first principles approach was adopted, whereby primary data underwent review and were tagged according to structure type in a 3D modelling environment. Thus individual mapping points, downhole photography intervals, interpreted photogrammetry and other datasets were assigned a structural category, resulting in a cloud of datapoints in 3D. These tagged datapoints were subsequently interrogated, and those that displayed similar structural characteristics and conformed with the understanding of the local geological and structural evolution were assigned to individual interpreted fault designations (see Section 3.4).

Data tagged to fault designations were used as direct inputs to construct individual faults and when combined with calculated averages for major structural groups, permitted the accurate delineation and modelling of individual single to multi-bench scale structures in 3D space. This approach allows for the rapid update of the interpretation as data become available and, once appropriately tagged, may be updated immediately.

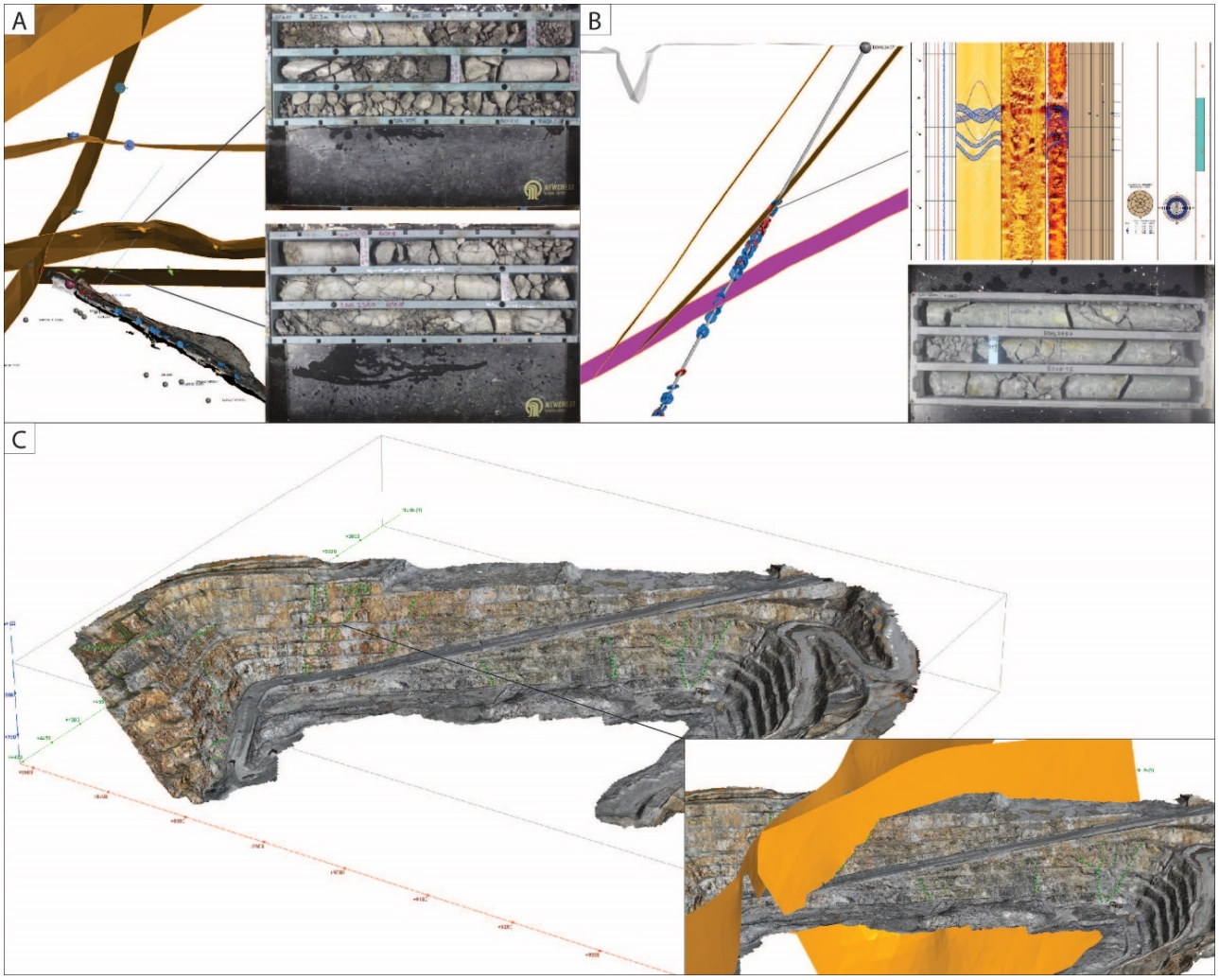

Figure 4 Examples of various datasets utilised for structural analysis: A) downhole core photographs used in conjunction with structural logging; B) downhole ATV/OTV data viewed in conjunction with core photographs; C) aerial photogrammetry assisting with the delineation of fault crosscutting relationships

3.2 Definition of principal structural systems

Ongoing open pit investigations indicate a protracted multistage structural evolution where structures (faults, shears and veins) have undergone several stages of activity and reactivation, but with largely consistent geometries and resultant trends. These principal trends are presented in Table 1.

Table 1 Principal structural trends at Lihir mine, compiled from works by Corbett (2012); Blackwell et al. (2014); Sykora (2016); Sykora et al. (2018); Lawlis (2020) and Newcrest mine staff

Trend	Associated stress regime/description
East–west low-angle structures	Early localised compression resulted in low-angle thrust faults and shear vein arrays with sub-horizontal dips. Linking these low-angle veins are sets of veins and breccias with high-angle dips (~65°) to the northwest.
East-northeast/ northeast to north–south	Combination of oblique structures produced by transposition and counterclockwise rotation of the Tabar-Lihir-Tanga-Feni island chain during north-westward migration over the past ~1 to 3 Ma. ENE-NE striking structural grain underpins Lihir Island, observed at both regional and deposit scales, and reactivated throughout the evolution of the deposit.
West-northwest-east-southeast	Early localised NW- and/or SE-directed compression and WNW-directed extension was linked with vein formation during early porphyry-style alteration under low differential stress, an oscillating sub-horizontal to sub-vertical σ1, and temporarily elevated fluid pressures from mineral sealing.
Northeast/east-northeast	Later stage fault and vein reactivation and modification. Multistage extension and top-block down to the northwest to north-northwest sense of shear along a system of interconnected veins with low-angle dips to the north. NW-directed extension with predominantly sub-vertical σ1 during extension.
East–west	Arcuate generally east–west-trending, north-dipping, listric-shaped structures associated with the collapse of the volcanic edifice.

Where sufficient data are available, structures conforming to these broad trends have been modelled.

3.3 Establishment of crosscutting relationships

Once principal trends have been identified and relevant kinematic controls defined, a wide hierarchy of crosscutting and terminating relationships between trend sets are established. This broadly establishes the anticipated relationship between modelled structures where they intersect, although this is reviewed and adjusted on a case-by-case basis as geological data allow, considering the possibility of reactivation along these structures. Field-based and photogrammetry-based mapping work was fundamental in the definition of timing relationships between interpreted structural systems (Figure 5).

3.4 Development of cohesive 3D interpretation

Once individual structures and principal trends were defined, and crosscutting relationships identified, a fully constrained interpretation was established. A fully constrained structural interpretation is essential for accurately understanding and, more importantly, predicting geological structures. Consideration of multiple lines of evidence ensures that interpretation is well-supported and consistent, reducing ambiguity and uncertainty. This further provides a comprehensive view of geological structures, highlighting relationships between different features and their spatial distribution. This further allows for the identification and analysis of key structural elements and their implications for geological processes, resource potential and engineering applications.

Incorporation of diverse datasets reduces the risk of misinterpretation or bias from relying on single data sources. Fully constrained interpretations further assist in identifying and understanding the controls on geological structures such as stress regimes, tectonic forces or stratigraphic variations. Understanding these controls is valuable for predicting the behaviour of subsurface formations including fluid flow pathways, reservoir properties and slope hazards. Moreover, a fully constrained interpretation facilitates effective communication and collaboration among geologists, engineers and client stakeholders by providing a clear and well-supported framework for decision-making and planning purposes. A standardised document referred to as the 'fault atlas' was developed to document and relay data inputs, structural and geotechnical characteristics, and crosscutting/terminating relationships with other modelled structures, providing a consistent framework for geological and civil works to operate within.

A mine-wide structural model has been developed in Leapfrog Geo (Seequent 2020), and is comprised of multi-bench scale structures and associated secondary structures. The model is supported with a fault atlas detailing the interpreted fault properties of each proposed fault wireframe, and was prepared to assist with ongoing slope stability assessment. The fault network has been established as a single coherent framework for ongoing studies, with a weight-of-evidence approach taken whereby fault models are updated/adjusted where data allow. The modelled fault network across the Lihir mine extent comprises 100 modelled structures at the time of writing (Figure 5).

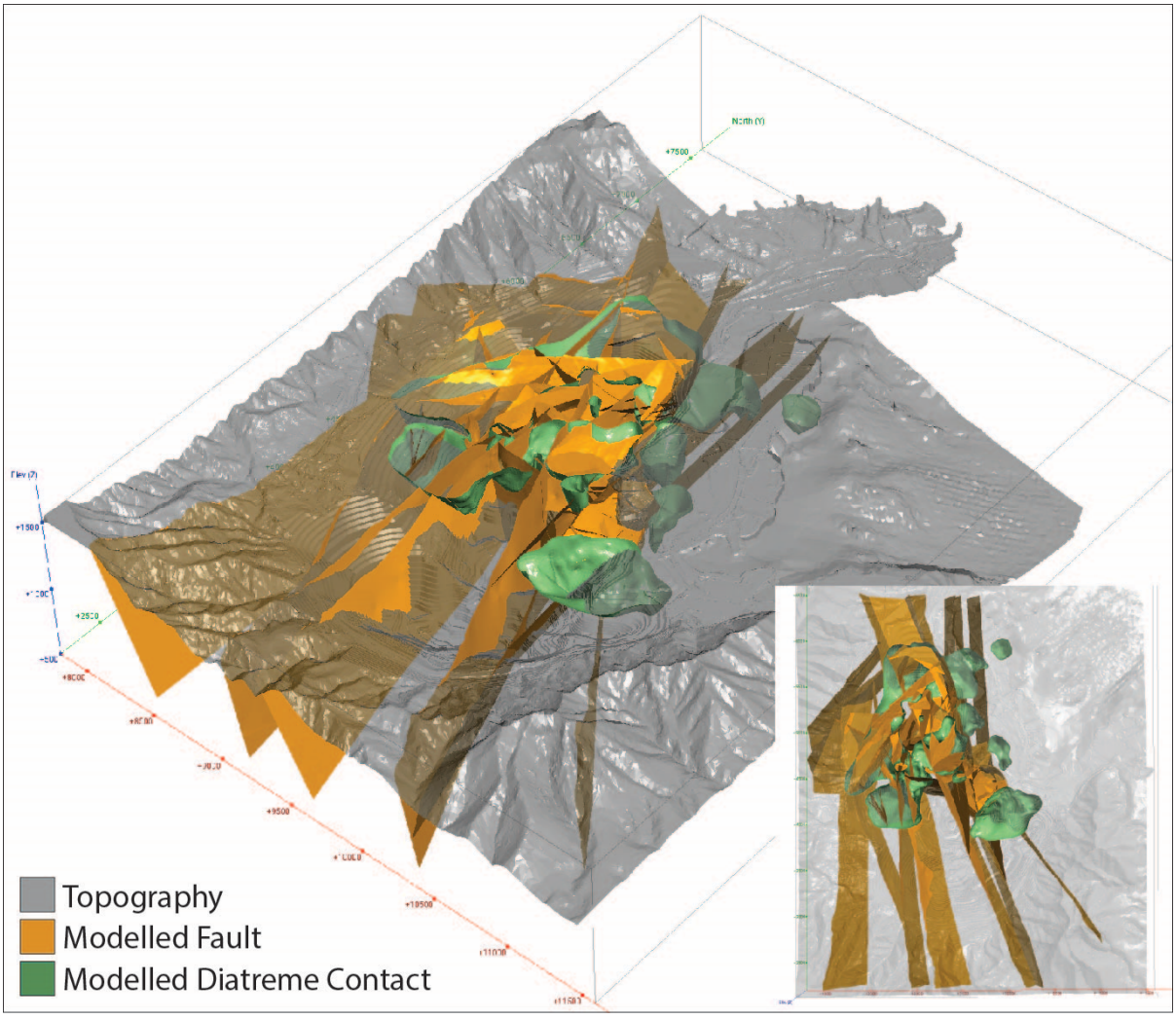

Figure 5 The modelled fault network across the Lihir mine project extent, incorporating all available geological, geophysical and geotechnical data

4 Utilisation in slope design

Continuous onsite data collection and corresponding updates to modelled structures allow for review of anticipated versus in situ ground conditions. The methodology allows for the rapid update and adjustment of modelled structures, integrated into a fully constrained interpretation based on observations made from supporting data as it becomes available.

Identified structures and structural trends are utilised in downstream kinematic slope stability analysis and allow for the opportunistic optimisation of slope designs. These structures are reviewed in 3D to investigate how they interact with the design slopes to identify and conceptualise any potential instability mechanisms that require evaluation. Localised adjustments to slope design can then be implemented where required based on this structural review (and rock mass assessments). This, in turn, may allow for optimisation of slopes where structural conditions are less adverse; particularly if the slope designs are governed by kinematics. Additionally, improving slope stability through the use of targeted anchors in areas where anticipated structures are expected to govern slope stability may be considered through a cost-benefit analysis to determine feasibility of these optimised designs.

5 Conclusion

A fully constrained structural interpretation provides a comprehensive and reliable understanding of geological structures and conditions, enhancing the efficiency and likelihood of success of geological investigations and subsequent engineering projects. A fully constrained structural model in slope design offers several advantages:

- Accurate identification of potential failure surfaces within the slope. This includes the identification of contact zones, faults and other structural features that may contribute to slope instability.
- Improved stability analysis, which provides a solid foundation for conducting stability analyses of slopes. By considering the orientation, spacing and nature of geological features, determination of slope stability under various loading conditions allows for the design of appropriate reinforcement measures.
- Incorporation of enhanced geotechnical design, which allows for a more comprehensive geotechnical design of slopes, enabling assessments of strength and behaviour of the various geological units, and considering unit geometries and interactions. Multiple iterations of design and sensitivity analysis provide accurate assessments of the slope's bearing capacity, shear strength and deformation characteristics, enabling the design of suitable slope stabilisation measures.
- Effective risk management, which provides a clearer understanding of potential failure mechanisms and their probability of occurrence. By considering the structural complexities of the slope, engineers can identify high-risk areas and develop targeted monitoring and mitigation strategies. This allows for proactive measures to be implemented, reducing the likelihood of slope failures and minimising potential consequences.
- Optimal resource allocation as resources may be allocated more efficiently during slope design and construction. By accurately characterising the geological structures, unnecessary excavation or reinforcement measures can be avoided in areas where the slope is inherently stable. This optimisation of resources helps reduce costs, increase project efficiency and improve overall design sustainability.

A fully constrained structural model in slope design offers advantages such as accurate identification of potential failure surfaces, improved stability analysis, enhanced geotechnical design, effective risk management and optimal resource allocation. These benefits contribute to the development of safe and cost-effective slope designs, reducing the potential for slope failures and ensuring the long-term stability of the slopes.

6 Acknowledgement

The authors acknowledge and thank Newcrest Mining Ltd for its logistical and technical support with the compilation of this paper.

References

Blackwell, JL 2010, *Characteristics and Origins of Breccias in a Volcanichosted Alkalic Epithermal Gold Deposit, Ladolam, Lihir Island, Papua New Guinea*, PhD thesis, University of Tasmania, Hobart.

Blackwell, JL, Cooke, DR, McPhie, J & Simpson, KA 2014, 'Lithofacies associations and evolution of the volcanic host succession to the Minifie ore zone, Ladolam gold deposit, Lihir Island, Papua New Guinea', *Economic Geology*, vol. 109, no. 4, pp. 1137–1190, https://doi.org/10.2113/econgeo.109.4.1137

Carman, GD 1994, *Genesis of the Ladolam Gold Deposit, Lihir Island, Papua New Guinea*, PhD thesis, Monash University, Melbourne.

Cole, JW, Milner, DM & Spinks, KD 2005, 'Calderas and caldera structures: a review', *Earth-Science Reviews*, vol. 69, no. 1–2, pp. 1–26, https://doi.org/10.1016/j.earscirev.2004.06.004

Cooke, D & Sykora, S 2020, 'Lihir Alkalic epithermal gold deposit, Papua New Guinea', in E Lawlis, J Blackwell, M Ageneau, N Jansen, A Harris & D Selley (eds), *Geology of the Yukon-Tanana Terrane and Adjacent Regions*, Society of Economic Geologists, Littleton, pp. 491–512.

Corbett, GJ 2012, 'Structural controls to, and exploration for, epithermal Au-Ag deposits', *Australian Institute of Geosciences Bulletin*, vol. 56, pp. 43–47.

Davies, RH & Ballantyne, GH 1987, 'Geology of the Ladolam gold deposit Lihir Island, Papua New Guinea', paper presented at Pacific Rim Congress 87, Gold Coast.

Gordon, RG, Cox, A & Harter, CE 1978, 'Absolute motion of an individual plate estimated from its ridge and trench boundaries', *Nature*, vol. 274, no. 5673, pp. 752–755, https://doi.org/10.1038/274752a0

Hall, R 2002, 'Cenozoic geological and plate tectonic evolution of SE Asia and the SW Pacific: computer-based reconstructions, model and animations', *Journal of Asian Earth Sciences*, vol. 20, no. 4, pp. 353–431, https://doi.org/10.1016/S1367-9120(01)00069-4

Holt, RM 1990, 'Permeability reduction induced by a nonhydrostatic stress field', *SPE Formation Evaluation*, vol. 5 no. 04, pp. 444–448, https://doi.org/10.2118/19595-PA

Lawlis, E 2020, *Geology of the Kapit NE and coastal ore zones, Lihir gold deposit, Papua New Guinea*, BSc Hons thesis, University Of Tasmania.

Lawlis, E, Cooke, DR & Harris, AC 2015, 'Volcanic-hydrothermal breccias at the Lihir alkalic gold deposits, Papua New Guinea', paper presented at 13th Biennial Society for Geology Applied to Mineral Deposits Meeting, Nancy.

Moyle, AJ, Doyle, BJ, Hoogvliet, H & Ware, AR 1990, 'Ladolam gold deposit, Lihir Island', Australasian Institute of Mining and Metallurgy, vol. 14, pp. 1793–1805.

Pichler, T, Giggenbach, WF, McInnes, BIA, Buhl, D & Duck, B 1999, 'Fe sulfide formation due to the seawater-gas-sediment interaction in a shallow-water hydrothermal system at Lihir Island, Papua New Guinea', Economic Geology, vol. 94, pp. 281–288, https://doi.org/10.2113/gsecongeo.94.2.281

Seequent 2020, *Leapfrog Geo*, computer software, Seequent, Christchurch, https://www.seequent.com

Sharp, WD & Clague, DA 2006, '50-Ma Initiation of Hawaiian-Emperor bend records major change in Pacific plate motion', *Science*, vol. 313, no. 5791, pp. 1281–1284, https://doi.org/10.1126/science.1128489

Simmons, SF & Brown, KL 2006, 'Gold in magmatic hydrothermal solutions and the rapid formation of a giant ore deposit', *Science*, vol. 314, no. 5797, pp. 288–291, https://doi.org/10.1126/science.1132866

Sykora, S 2016, *Origin, Evolution and Significance of Anhydrite-Bearing Vein Arrays and Breccias, Lienetz Orebody, Lihir Gold Deposit, Papua New Guinea*, PhD thesis, University of Tasmania, Hobart.

Sykora, S, Selley, D, Cooke, DR & Harris, AC 2018, 'The structure and significance of anhydrite-bearing vein arrays, Lienetz orebody, Lihir Gold Deposit, Papua New Guinea', *Economic Geology*, vol. 113, no. 1, pp. 237–270, https://doi.org/10.5382/econgeo.2018.4550

Tregoning, P 2002, 'Plate kinematics in the western Pacific derived from geodetic observations', *Journal of Geophysical Research, Solid Earth,* vol. 107, no. B1, pp. 71–78, https://doi.org/10.1029/2001JB000406

Wallace, DA, Johnson, RW, Chappell, BW, Arculus, RJ, Perfit, MR & Crick, IM 1983, 'Cainozoic volcanism of the Tabar, Lihir, Tanga, and Feni Islands, Papua New Guinea: Geology whole-rock analyses and rock-forming mineral compositions', *Australian Bureau of Mineral Resources, Geology and Geophysics*, vol. 243, no. MF197, pp. 1–140, https://www.scopus.com/record/display.uri?eid=2-s2.0-0020862124&origin=inward&txGid=fd0389a1469900f79323dd1b334749eb